The influence of a mini-magnetopause on the magnetic pileup boundary at Mars

E. M. Harnett
Department of Earth and Space Sciences, University of Washington, Seattle, Washington, USA

R. M. Winglee
Department of Earth and Space Sciences, University of Washington, Seattle, Washington, USA

Received 28 May 2003; revised 17 September 2003; accepted 3 October 2003; published 31 October 2003.

[1] 3D single fluid non-ideal MHD simulations are used to predict positions for the bow shock and magnetic pileup boundary (MPB). The positions are in agreement with those calculated from Mars Global Surveyor data. The simulations were run with the strong southern magnetic anomalies facing into the solar wind, and the IMF in either the northward or southward direction. The simulations show that the strong southern magnetic anomalies create a magnetopause-like structure (i.e., a mini-magnetopause) in place of an MPB but plasma signatures for both types of boundaries are similar. Distinguishing characteristics include the magnetic field orientation, pressure, and the current. The current regions associated with a mini-magnetopause are larger in scale and greater in magnitude than those at the MPB. The simulations also show that including non-ideal MHD physics is important in resolving both the magnetic pileup boundary and the mini-magnetopause. *INDEX TERMS:* 2740 Magnetospheric Physics: Magnetospheric configuration and dynamics; 2753 Magnetospheric Physics: Numerical modeling; 2756 Magnetospheric Physics: Planetary magnetospheres (5443, 5737, 6030); 6225 Planetology: Solar System Objects: Mars. **Citation:** Harnett, E. M., and R. M. Winglee, The influence of a mini-magnetopause on the magnetic pileup boundary at Mars, *Geophys. Res. Lett.*, *30*(20), 2074, doi:10.1029/2003GL017852, 2003.

1. Introduction

[2] Mars Global Surveyor has detected a bow shock and magnetic pile-up boundary (MPB) located respectively at 0.7 R_M and approximately 1200 km from the surface [cf. *Vignes et al.*, 2000]. An MPB exists near any non-magnetized, comet-like object which has a dense and extended atmosphere/ionosphere [cf. *Mazelle et al.*, 1989]. As the interplanetary magnetic field (IMF) meets a high conductivity planetary plasma the IMF begins to pile-up. At Mars, the MPB is also a region where solar wind ions undergo charge exchange with exospheric neutrals [*Riedler et al.*, 1989] and solar wind electrons rapidly lose energy through impact ionization with exospheric neutrals [*Crider et al.*, 2000]. The transition from outside the MPB to inside appears as an increase in the magnitude of the magnetic field, a decrease in the magnetic field fluctuations and a simultaneous sharp decrease in the high energy (solar wind) electron flux [*Vignes et al.*, 2000], as solar wind electrons begin ionizing planetary hydrogen and oxygen [*Crider et al.*, 2000].

[3] *Crider et al.* [2002] found that the location of the MPB shows both latitudinal and longitudinal dependence. The average height of the MPB was 200 km higher on the day-side southern hemisphere than the day-side northern hemisphere. In the southern hemisphere, where the strong magnetic anomalies are located (*Acuna et al.* [1999] and *Connerney et al.* [1999]), the average MPB height in the vicinity of the largest magnetic anomalies is both 140 km higher than outside the anomalous region and more variable.

[4] *Ma et al.* [2002] conducted 3D ideal MHD simulations of the Martian magnetosphere, using a magnetized Mars, to investigate the effects of the hot oxygen corona on the locations of the ionopause and bow shock. They found that the position of the ionopause was approximately 100 km further from the surface over the southern hemisphere than the northern hemisphere due to the anomalous magnetic field. But their model could not resolve the magnetic pileup boundary and did not make any predictions about possible mini-magnetopauses.

[5] This paper presents results from a single fluid, non-ideal MHD model of the solar wind interaction with the magnetic anomalies at Mars. The non-ideal MHD aspect allows the model to capture the particle type effects occurring within the magnetosphere and resolve the magnetic pileup boundary. The simulation presents evidence for the formation of mini-magnetopauses in place of a magnetic pileup boundary when the strongest anomalies are on the dayside. The simulation results enable us to determine diagnostics to differentiate between various boundaries, as the signature for crossing a mini-magnetopause would be similar to crossing the MPB.

2. Model

[6] The simulation solves the following equations in 3D on a nested grid system, with 3 grids centered about the equator and noon meridian. The resolution of the finest grid is 109 km, and 435 km in the coarsest grid.

$$\frac{\partial \rho_m}{\partial t} + \nabla \cdot \mathbf{m} = 0 \tag{1}$$

$$\frac{\partial \mathbf{m}}{\partial t} + \nabla \cdot \left(\mathbf{m} \frac{\mathbf{m}}{\rho_m} \right) + \nabla P = \mathbf{J} \times \mathbf{B} + \rho_m \mathbf{g}(\mathbf{r}) \tag{2}$$

0094-8276/03/2003GL017852$05.00

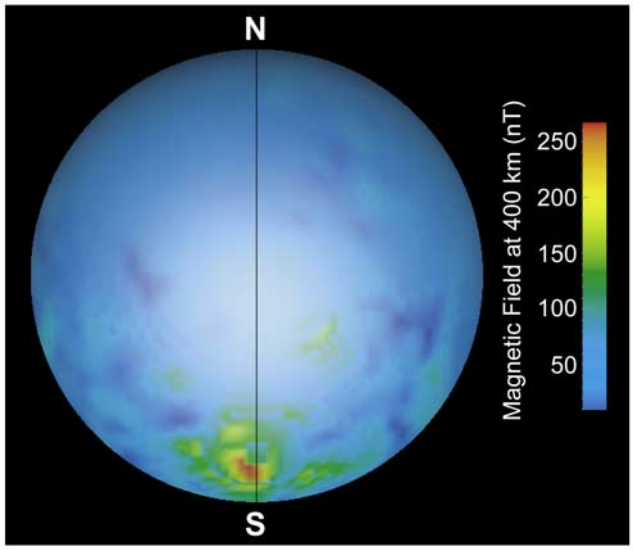

Figure 1. The simulated Martian magnetic field at 400 km from the surface. The black line indicates the noon meridian and the location of the 2D cuts shown in Figures 2 and 3. The equatorial plane is aligned with the ecliptic plane. The black line also corresponds to the location of 180°E longitude. From the model provided by *Cain et al.* [2003].

$$\frac{\partial \mathrm{e}}{\partial t} + \nabla \cdot \left(\frac{\mathbf{m}}{\rho_m} (\mathrm{e} + \mathrm{P}) \right) = \mathbf{E} \cdot \mathbf{J} + \mathbf{m} \cdot \mathbf{g}(\mathbf{r}) \tag{3}$$

$$\frac{\partial \mathbf{B}}{\partial t} + \nabla \times \mathbf{E} = 0 \tag{4}$$

$$\mathbf{J} = \nabla \times \mathbf{B} \tag{5}$$

$$\mathbf{E} = -\mathbf{v} \times \mathbf{B} + \eta \mathbf{J} + \frac{c}{\omega_{pi} \mathrm{L} \rho_\mathrm{m}} (\mathbf{J} \times \mathbf{B} - \nabla P e) \tag{6}$$

where ρ_m is the mass density of the ion population, **m** is the bulk momentum, **v** is the bulk velocity, e is the energy density, **g**(**r**) is the gravitational vector, **J** is the current, **B** is the magnetic field, **E** is the electric field, P_e is the electron pressure (and half the total pressure, P), η is the resistivity of Mars, c is the speed of light, L is the scale size of the grid, and ω_{pi} is the hydrogen ion plasma frequency. The resistivity (η) is non-zero only inside the simulation planetary boundary and the Hall and ∇P_e terms are only evaluated outside the boundary.

[7] Ohm's Law is given in dimensionless units with the ratio c/ω_{pi} equal to the ion inertial length. The ratio $c/(\omega_{pi}L)$ is a measure of the strength of particle-like effects. In the simulations, $c/(\omega_{pi}L)$ is equal to 0.3, but reduced to 0.1 for stability of the calculations. This is still sufficient to capture particle type effects, such as localized charge separation and ion demagnetization as shown by *Winglee* [1994] where $c/(\omega_{pi}L)$ was reduced by a similar percentage. As $c/(\omega_{pi}L)$ is increased from zero towards 0.3, any boundaries associated with Hall or pressure gradient terms will sharpen and the magnitude of the electric field in that region will increase. More detailed discussions of the non-ideal MHD terms and a comparison between self-consistent particle simulations and non-ideal MHD fluid simulations of both the Earth's magnetosphere and mini-magnetospheres at the Moon can be found in *Winglee* [1994] and *Harnett and Winglee* [2002] respectively.

[8] The non-ideal treatment also provides an inherent scale length, unlike ideal MHD where no inherent scale length exists and boundaries such as the bow shock will be three grid points thick, regardless of the resolution. In non-ideal MHD the ion cyclotron radius sets the inherent scale length and boundaries 3 grid points thick are just unresolved.

[9] The solar wind density is 4 ions cm^{-3}, with a speed of 400 km s^{-1}. The IMF is only in the B_z direction with a magnitude of 1 nT. The coordinates are such that $\vec{z}$ is perpendicular to the ecliptic plane, $\vec{y}$ is in the ecliptic plane but perpendicular to the solar wind velocity, and $\vec{x}$ is parallel to the solar wind velocity.

[10] Viking 1 measured the density of O_2^+ at 300 km to be approximately 200 cm^{-3}, while the maximum O_2^+ density of 10^5 cm^{-3} occurred at 130 km [*Hanson et al.*, 1977]. The simulation planetary boundary is defined as 300 km above the surface with a number density of 100 O_2^+ cm^{-3} and a temperature of 3000 K held constant throughout the simulation. As this is a single fluid simulation, one O_2^+ ion is treated as 32 H^+ ions in setting the mass density at the boundary. Increasing the density and temperature beyond these values can lead to strong outflows from the planet that will produce an inflated magnetosphere.

[11] The model of the Martian magnetic field was provided by *Cain et al.* [2003]. A 90 term internal potential function was generated using 110,000 3-component observations. Figure 1 shows a map of the magnitude of the magnetic field at 400 km from the surface (and 100 km above the simulation boundary). In the simulations the strong southern magnetic anomalies face directly into the solar wind. The black line in Figure 1 indicates the noon meridian and the location of the 2D cuts shown in Figures 2 and 3 as well as the location of 180°E longitude on the

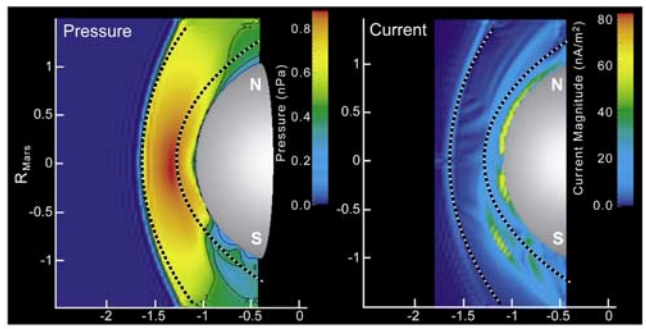

Figure 2. The pressure and current in the plane through the noon meridian for southward IMF. The black contour lines in (a) are at the values of 0.22, 0.35, and 0.47 nPa. The silver sphere represents the inner boundary of the simulations at an altitude of 300 km. The plane shown contains an area 7285 km by 10330 km, with a grid resolution of 109 km. The black and white curves indicate the position of the bow shock and magnetic pileup boundary as calculated by *Vignes et al.* [2000].

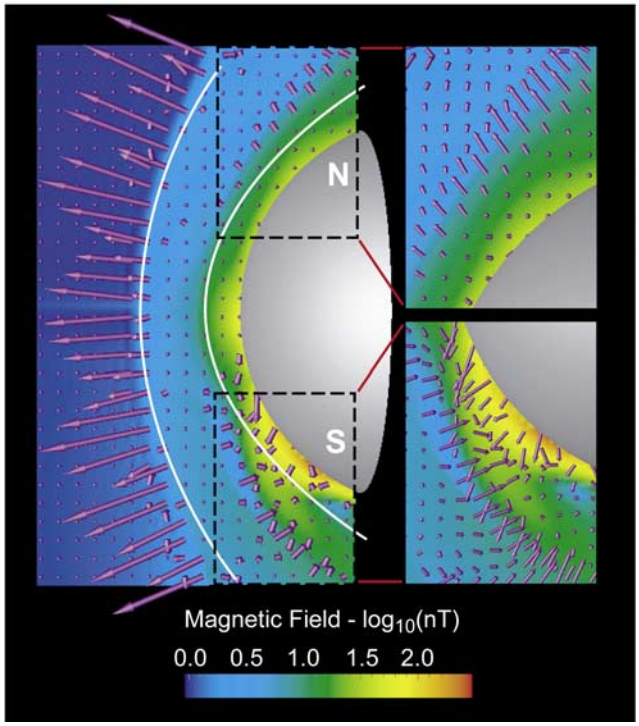

Figure 3. The electric field vectors and the magnitude of the magnetic field in the plane running through the noon meridian for southward IMF. The electric field out of the plane has been set to zero. The maximum electric field vector size is equal to 0.37 mV/m and vectors with a magnitude below 0.015 mV/m were set to zero. The silver sphere represents the inner boundary of the simulations. The white curves indicate the positions of the bow shock and MPB as calculated by *Vignes et al.* [2000].

surface. For these results, the equatorial plane is aligned with the ecliptic plane.

3. Results

[12] The subsolar point of the bow shock forms at 0.63 R_M for the southward IMF in the simulations, and about 0.03 R_M (or one grid point) further out for northward IMF, in agreement with the average position of the subsolar point of 0.64 ± 0.08 R_M as calculated by *Vignes et al.* [2000]. Figure 2 shows the pressure and current in the noon meridian for southward IMF, with the black and white curves indicating the position of the bow shock and the MPB as calculated by *Vignes et al.* [2000]. They used 450 bow shock and 488 MPB crossings from Mars Global Surveyor to produce the fits. As such, the fits are for an average over a range of solar wind conditions, not the position for one particular solar wind condition. The discrepancy between the measured and simulation bow shock position at the flanks could be due to both the fact that the predicted shape from MGS is an average and therefore the fit parameters have inherent uncertainty, and the lower density used for the planetary boundary.

[13] The fits by *Vignes et al.* [2000] put the position of the magnetic pileup boundary at 0.29 ± 0.04 R_M from the surface at the nose and is indicated by the inner black and white curve in Figure 2. The MPB can not be seen in the pressure plots. But a magnetopause-like pressure boundary can be seen in the southern hemisphere above the location of the magnetic anomalies.

[14] The magnetic pileup boundary can be seen in the simulation magnetic and electric field. Figure 3 shows the magnitude of the magnetic field and the electric field vectors in the noon meridian. The component of the electric field out the plane has been set to zero for clarity. The MPB can be seen as an increase in the magnetic field strength by an order of magnitude. The electric field in the northern hemisphere indicates that more than IMF pileup is occurring at the MPB.

[15] Associated with the MPB is an electric field pointing away from the surface, in the same direction as the electric field at the bow shock. The electric field at the bow shock is due to solar wind ions penetrating further into the shock as a result of their larger momentum, creating an electric field pointing into the solar wind. This is captured by the ∇P_e term in Equation 6. The direction of the electric field vectors at the MPB indicates there is an excess of electrons or deficit of ions in comparison to the region just below. At the MPB, the Hall term in Equation 6 is responsible for the direction of the electric field in the plane through the noon meridian and dominates over the pressure gradient term. The Hall term indicates the occurrence of non-ideal MHD behavior. The large Hall component of the electric field at the MPB indicates that ion demagnetization occurs at the boundary, with the demagnetized ions penetrating further into the ionosphere than the electrons which remain tied to the magnetic field and pile up. Ion demagnetization due to non-ideal MHD effects was seen in 2.5D simulations of mini-magnetospheres at the Moon [*Harnett and Winglee*, 2002].

[16] The mini-magnetopause that forms in the southern hemisphere can be seen in the electric and magnetic field as well as the pressure and current. The boundary forms around 0.4 R_M, as measured radially out from the strongest anomalies (0.41 R_M for southward IMF and 0.38 R_M for northward IMF), about 200 to 300 km higher than the MPB would form in the absence of anomalous magnetic field. The mini-magnetopause is different from the MPB in that there is a large gradient in the thermal pressure. As the thermal pressure decreases inside the mini-magnetopause another form of pressure, namely magnetic pressure increases to balance the total pressure at a boundary that is further away from the surface. Inside the mini-magnetopause, multiple current systems form due to the complex geometry of the total magnetic field.

[17] Reconnection of the IMF to the anomalous magnetic field changes the shape of the mini-magnetopause. The total magnetic field is reduced outside the mini-magnetopause boundary for northward IMF, indicating increased reconnection to the anomalous magnetic field to the IMF. The direction of the magnetic field in the extended loop structures determines the extent of reconnection to the IMF. The radial portion of the magnetic field plays a large role in determining the internal structure of the mini-magnetopause. And while the bulk of the IMF is generally in the B_y direction at Mars, the simulations show that the B_z component of the IMF plays a large role in shaping the mini-magnetopause. Changes in the direction of B_z may

lead to dynamics, similar to that seen at the Earth's magnetosphere.

[18] At the mini-magnetopause boundary, the pressure gradient is comparable in magnitude to the Hall term, unlike at the MPB where the pressure gradient term is small across the boundary. The electric field vectors change direction going across the mini-magnetopause boundary (Figure 3). This is due to the change in dominance of the Hall and the pressure gradient terms. The Hall component of the electric field points away from the planet while the pressure gradient points toward the planet. The pressure gradient points inward because the boundary is magnetopause-like. The mini-magnetopause demarcates the boundary that separates hot magnetosheath plasma and cold ionospheric plasma. The strength of the Hall component indicates that ion demagnetization is occurring as well.

4. Discussion

[19] The simulations predict that over the strongest magnetic anomalies, a mini-magnetopause forms in place of the MPB. Both boundaries would appear similar in particle flux measurements though. At the MPB, the solar wind mixes with the Martian ionosphere, becoming indistinguishable from ionospheric populations. At the mini-magnetopause, the anomalous magnetic field deflects the solar wind, preventing access. Thus crossing both types of boundaries will lead to a "disappearance" of the solar wind, albeit through different mechanisms. The mini-magnetopause forms at a higher altitude only in some cases, such as those presented here where the strongest anomalous magnetic field is on the dayside.

[20] Distinguishing characteristics may be found in the magnetic field. At both boundaries the magnitude of the magnetic field increases but greatest at the mini-magnetopause. Once inside the MPB, the magnetic field magnitude will still increase but do so slowly, and then fall off sharply at the ionopause. Inside the mini-magnetopause, the magnetic field magnitude will increase by at least an order of magnitude. At the MPB, only small changes in the angle of the magnetic field will occur due to draping of the IMF. At the mini-magnetopause, the magnetic field orientation will exhibit large angle changes. The rapid fluctuations in the magnetic field orientation in the magnetosheath prior to crossing the MPB or mini-magnetopause may make this a problematic signature to find though.

[21] Further differences come about when looking at moment data and current. The simulations show a large pressure gradient only at the mini-magnetopause. But this strong asymmetry between the pressure at the mini-magnetopause and the MPB is not prominent in either the temperature or density alone. And the current (Figure 2) is three to four times larger in magnitude at the mini-magnetopause.

[22] The structure of the current systems is also substantially different. The current at the MPB is distributed along a 300 km thick boundary. At the mini-magnetopause, on the other hand, a current system is present throughout a 600–1200 km thick region. Inside the mini-magnetopause additional current systems are present and of comparable magnitude to the current densities at the mini-magnetopause. So not only is the magnitude of the current stronger at the mini-magnetopause, a strong current signal is present throughout the entire region. For northward IMF, only the internal structure of the current changes.

[23] Two criteria determine if these boundaries are resolved and significant, the ion cyclotron radius at the boundary and the thickness in grid points. The ion cyclotron radius at the MPB varies between 60 km at the outer edge and 10 km at the inner edge. But with a thickness of three grid points, the MPB is not completely resolved and could be thinner than the 300 km indicated by the model. The current system at the mini-magnetopause is 5–12 grid points in size and therefore the boundary and structures are well resolved. The ion cyclotron radius at the mini-magnetopause varies between 80 km and 10 km, and even smaller inside mini-magnetopause. Only near the strongest current region is the ion cyclotron radius comparable to the grid size at 200 km. Thus the structure of the current systems inside the mini-magnetopause are not likely to change substantially with higher resolution.

[24] The results show that non-ideal MHD effects are significant inside the Martian magnetosphere and that ion demagnetization occurs at both the MPB and the mini-magnetopause. As such, the non-ideal MHD effects must be included in a model to begin to capture the physics occurring at the magnetic pileup boundary and the mini-magnetopause.

[25] Comparison of the MPB location in the northern hemisphere for a magnetized and unmagnetized Mars, shows little change for both northward and southward IMF. But near the equator, the MPB does form $\sim$150 km further from the surface for a magnetized Mars. Thus the simulations agree with the results from *Crider et al.* [2002] indicating that the magnetic anomalies can cause the MPB to form at higher altitudes. There are two caveats though. In the simulations a mini-magnetopause can form in place of an MPB. And for the results presented by *Crider et al.* [2002], MGS was at a solar zenith angle greater than 70° when measuring MPB locations in the southern hemisphere [*D. Crider*, private communication, 2002]. The results presented in this paper analyze the plasma properties at a solar zenith angle of 0°.

[26] The next step in development of the model will be to account for multiple fluids. A multi-fluid treatment will allow for a mass difference between the solar wind ion and ionospheric plasma. Modeling the Martian ionosphere with heavy ions will also increase the gravitational binding of the ionosphere, allowing for a lower altitude simulation boundary and study of the effect of the anomalous magnetic field on the ionopause. The ionopause currently sits at the simulation boundary over the unmagnetized regions. This will also be a natural place to loosen the assumption that the electron pressure is half the total pressure, and vary it over a range of values consistent with the system.

[27] **Acknowledgments.** The authors would like to thank J. C. Cain for providing the source code to generate the model Martian magnetic field, D. Crider for the helpful discussions about the Martian MPB, and L. Rachmeler for assistance in generating the figures in the paper. This research was supported by a NASA Graduate Student Research Fellowship, NASA grant NAG 5-11869, and NSF grant ATM-0105032.

References

Acuna, M. H., et al., Global Distribution of Crustal Magnetization Discovered by the Mars Global Surveyor MAG/ER Experiment, *Science*, *284*, 790–793, 1999.

Cain, J. C., et al., An n = 90 internal potential function of the Martian crustal magnetic field, *J. Geophys. Res.*, *102*(E2), doi:10.1029/2000JE001487, 2003.

Connerney, J. E. P., et al., Magnetic Lineations in the Ancient Crust of Mars, *Science*, *284*, 794–798, 1999.

Crider, D. H., et al., Evidence of electron impact ionization in the magnetic pileup boundary of Mars, *Geophys. Res. Lett.*, *27*, 45–48, 2000.

Crider, D. H., et al., Observations of the latitude dependence of the location of the Martian magnetic pileup boundary, *Geophys. Res. Lett.*, *29*, doi:10.1029/2001GL013860, 2002.

Hanson, W. B., et al., The Martian ionosphere as observed by the Viking retarding potential analyzers, *J. Geophys. Res.*, *82*, 4351–4363, 1977.

Harnett, E. M., and R. M. Winglee, 2.5D particle and MHD simulations of mini-magnetospheres at the Moon, *J. Geophys. Res.*, *107*, doi:10.1029/2002JA009241, 2002.

Ma, Y., et al., 3D multi-species MHD studies of the Solar Wind Interaction with Mars in the Presence of Crustal Fields, *J. Geophys. Res.*, *107*, doi:10.1029/2002JA009293, 2002.

Mazelle, C., et al., Analysis of suprathermal electron properties at the magnetic pile-up boundary at Comet P/Halley, *Geophys. Res. Lett.*, *16*, 1035–1038, 1989.

Riedler, W. D., et al., Magnetic field near Mars, *Nature*, *341*, 604–607, 1989.

Vignes, D., et al., The solar wind interaction with Mars: Locations and shapes for the bow shock and the magnetic pile-up boundary from the observations of the MAG/ER experiment onboard Mars Global Surveyor, *Geophys. Res. Lett.*, *27*, 49–52, 2000.

Winglee, R. M., Non-MHD influences on the magnetospheric current system, *J. Geophys. Res.*, *99*, 13,437–13,454, 1994.

E. M. Harnett and R. M. Winglee, Department of Earth and Space Science, Box 351310, University of Washington, Seattle, WA 98195-1310, USA. (eharnett@ess.washington.edu; winglee@ess.washington.edu)